Matrix metalloproteinase-13 mediated degradation of hyaluronic acid-based matrices orchestrates stem cell engraftment through vascular integration

Amit K. Jha [a, b], Kevin M. Tharp [c], Shane Browne [a, b, d], Jianqin Ye [e], Andreas Stahl [c], Yerem Yeghiazarians [e, f, g], Kevin E. Healy [a, b, *]

[a] Department of Bioengineering, University of California, Berkeley, CA 94720, USA
[b] Department of Material Science and Engineering, University of California, Berkeley, CA 94720, USA
[c] Department of Nutritional Science and Toxicology, University of California, Berkeley, CA 94720, USA
[d] Centre for Research in Medical Devices (CÚRAM), National University of Ireland Galway, Ireland
[e] Department of Medicine, University of California, San Francisco, CA 94143, USA
[f] Eli and Edythe Broad Center of Regeneration Medicine and Stem Cell Research, University of California, San Francisco, CA 94143, USA
[g] Cardiovascular Research Institute, University of California, San Francisco, CA 94143, USA

ARTICLE INFO

ABSTRACT

A critical design parameter for the function of synthetic extracellular matrices is to synchronize the gradual cell-mediated degradation of the matrix with the endogenous secretion of natural extracellular matrix (ECM) (e.g., creeping substitution). In hyaluronic acid (HyA)-based hydrogel matrices, we have investigated the effects of peptide crosslinkers with different matrix metalloproteinases (MMP) sensitivities on network degradation and neovascularization in vivo. The HyA hydrogel matrices consisted of cell adhesive peptides, heparin for both the presentation of exogenous and sequestration of endogenously synthesized growth factors, and MMP cleavable peptide linkages (i.e., QPQGLAK, GPLGMHGK, and GPLGLSLGK). Sca1$^+$/CD45$^-$/CD34$^+$/CD44$^+$ cardiac progenitor cells (CPCs) cultured in the matrices with the slowly degradable QPQGLAK hydrogels supported the highest production of MMP-2, MMP-9, MMP-13, VEGF$_{165}$, and a range of angiogenesis related proteins. Hydrogels with QPQGLAK crosslinks supported prolonged retention of these proteins via heparin within the matrix, stimulating rapid vascular development, and anastomosis with the host vasculature when implanted in the murine hindlimb.

© 2016 Elsevier Ltd. All rights reserved.

1. Introduction

Although stem cell based therapies are widely recognized as having the potential to regenerate damaged or diseased tissues including cardiac, skeletal muscle, and liver, substantial cell death and poor engraftment upon transplantation have limited the success of stem cell therapies [1—5]. In view of these issues, we have proposed that Matrix-Assisted Cell Transplantation (MACT) might be used to promote pro-survival autocrine/paracrine signaling and to enhance engraftment [6,7]. The design of synthetic matrices for cell transplantation includes biochemical and mechanical factors that promotes cell adhesion, proliferation, and differentiation, and stimulates engraftment of donor cells and tissue regeneration. They also require tunable strategies for controlled matrix degradation such as hydrolytically degradable linkages including lactic acid [8,9], epsilon-caprolactone [10], fumarate [11,12], and phosphoester [13]. With these materials, the degradation of the matrix occurs through non-specific bulk and/or surface erosion mechanisms, which are not always coordinated with the kinetics of tissue regeneration. As an alternative to these degradation strategies, cell-mediated matrix degradation has been pursued since it occurs in a temporal and spatial manner in concert with natural ECM formation [14—18].

Matrix metalloproteinases (MMPs) cleavable peptides have been targeted as ideal crosslinkers in synthetic matrices since they actively enhance tissue regeneration mediated by either transplanted or host cells [19—26]. The majority of these protease-degradable matrices have been fabricated by crosslinking with

only a small number of MMP-based peptide linkers, most commonly GPQGIAGQ or GPQGIWGQ [17,18,27,28], although rapidly degradable linkers have been used such as VPMSMRGG [22,23,29]. Hence the current paradigm is that synthetic matrices generated with MMP-sensitive peptide crosslinkers exhibiting defined Michaelis−Menten parameters (k_{cat}/K_m) will maintain a balance between cell-mediated degradation of the synthetic matrix and endogenously synthesized ECM, thus supporting cell survival and stimulating engraftment via synchronous remodeling of the synthetic matrices in concert with ECM formation [22,23,25]. However, a systematic analysis of MMP degradable crosslinkers in synthetic matrices for stem cell transplantation, and subsequent angiogenesis, has not been studied.

In this work, we studied the biological outcomes of cell laden synthetic hydrogel matrices with varied degradation kinetics in response to cell-induced MMP remodeling. We employed a previously described HyA hydrogel system [6,7], using high molecular weight HyA, a biopolymer with good biological performance that has been shown to also exhibit anti-inflammatory properties [30,31]. This matrix contains the 15 amino-acid bone sialoprotein-derived peptide containing the Arg-Gly-Asp (RGD) sequence bsp-RGD (15) (CGGNGEPRGDTYRAY) for cell adhesion, high molecular weight heparin (HMWH) for exogenously added and endogenously synthesized growth factor presentation [6], and contains MMP-cleavable peptide linkages that allows MMP-dependent remodeling of the matrix. A population of Sca1+/CD45−/CD34+/CD44+ cardiac progenitor cells (CPCs) that has demonstrated therapeutic capacity in a mouse ischemia model was used in our experiments [32]. This population of CPCs has tri-lineage potential to differentiate into cardiomyocytes, smooth muscle cells, and endothelial cells under the appropriate media conditions. CPCs cultured within our matrices containing HMWH and transforming growth factor beta 1 (TGFβ1) have demonstrated the formation of vascular-like structures both *in vitro* and *in vivo*.

Specifically, the presence of HMWH supports trophic functions of the CPCs by sequestering multiple endogenously secreted angiogenic factors within the matrix [6,7,33]. To test the effect of MMP degradation kinetics on CPC engraftment, three matrices were synthesized using the MMP-sensitive peptide crosslinkers (QPQGLAK, GPLGMHGK, and GPLGLSLGK) with significantly different degradation kinetics [25] (Table 1) (Fig. 1). We compared CPCs survival, proliferation, differentiation, and matrix production within the hydrogels *in vitro*. The matrix crosslinked with the slowest degradation kinetics (QPQGLAK) supported the highest secretion of MMP-13, VEGF$_{165}$, and angiogenesis related proteins. It also supported prolonged retention of these proteins and stimulated rapid vascular development. Compared to the other crosslinked matrices, *in vivo* studies revealed that matrices crosslinked
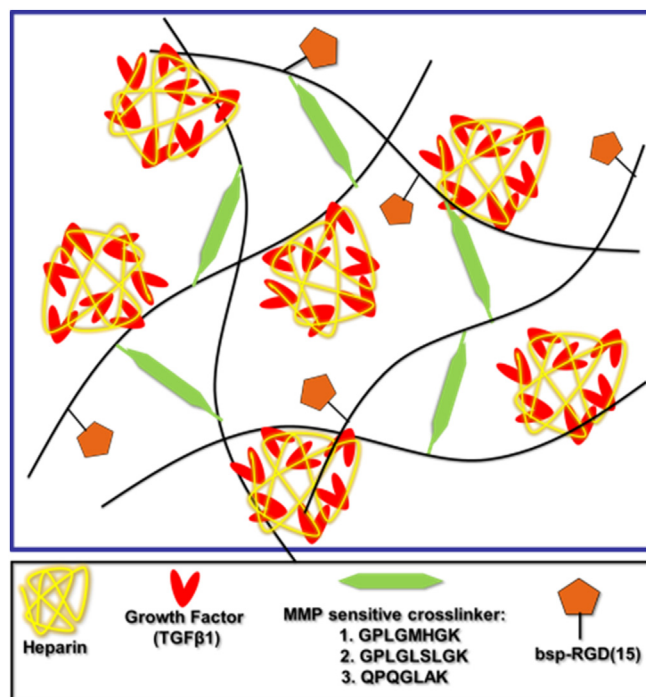
Fig. 1. Schematic of gel synthesis. HyA hydrogels containing cell adhesive bsp-RGD (15) peptide and heparin as a growth factor presenting agent were synthesized by crosslinking with matrix metalloproteinase (MMP)-cleavable peptides (QPQGLAK, GPLGMHGK, and GPLGLSLGK) of distinctly different Michaelis−Menten k_{cat}/K_m parameters.

with QPQGLAK significantly stimulated more robust angiogenesis and anastomosis of newly formed vessels with the host circulatory system.

2. Materials and methods

2.1. Materials

Hyaluronic acid (HyA, sodium salt, 500 kDa) was purchased from Lifecore Biomedical (Chaska, MN). Adipic dihydrazide (ADH), 1-ethyl-3-[3-(dimethylamino)propyl] carbodiimide (EDC), sodium hydroxide (NaOH), hydrochloric acid (HCl), tris(2-carboxyethyl) phosphine (TCEP), triethanolamine-buffer (TEOA; 0.3 M, pH 8) and 1-hydroxybenzotriazole (HOBt) were purchased from Aldrich (Milwaukee, WI). Dimethyl sulfoxide (DMSO), N-Acryloxysuccinimide (NAS) and, acetone ethanol were obtained from

Table 1
Kinetic parameters for MMP cleavable peptides (adapted from Reference [25]).

		QPQGLAK	GPLGLSLGK	GPLGMHGK
MMP-13	k_{cat} =	0.82 s^{-1}	14.10 s^{-1}	73.90 s^{-1}
	K_m =	1.10 μM	317.00 μM	465.00 μM
	k_{cat}/K_m	7.5 s^{-1} M^{-1}	4.4 e4 s^{-1} M^{-1}	1.6 e5 s^{-1} M^{-1}
	Normalized Ratio for k_{cat}/K_m	**1.00**	**60.00**	**213.00**
MMP-9	k_{cat} =	25.40 s^{-1}	46.70 s^{-1}	167.80 s^{-1}
	K_m =	1223.00 μM	940.00 μM	727.00 μM
	k_{cat}/K_m	2.1 e4 s^{-1} M^{-1}	5.0 e4 s^{-1} M^{-1}	2.3 e5 s^{-1} M^{-1}
	Normalized Ratio for k_{cat}/K_m	**1.00**	**2.00**	**11.00**
MMP-2	k_{cat} =	36.50 s^{-1}	21.10 s^{-1}	620.00 s^{-1}
	K_m =	2028.00 μM	216.00 μM	3558.00 μM
	k_{cat}/K_m	1.8 e4 s^{-1} M^{-1}	98000.00 s^{-1} M^{-1}	1.7 e5 s^{-1} M^{-1}
	Normalized Ratio for k_{cat}/K_m	**1.00**	**5.00**	**10.00**

Fisher Scientific (Waltham, MA). Dialysis membranes (10,000 MWCO, SpectraPor Biotech CE) were purchased from Spectrum Laboratories (Rancho Dominguez, CA). Paraformaldehyde (16% in H₂O) was obtained from Electron Microscopy Sciences (Hartfield, PA). High molecular weight heparin (HMWH) was obtained from Santa Cruz Biotechnology, Inc (Dallas, Texas). The MMP-degradable crosslinker peptides (CQPQGLAKC, CGPLGMHGKC, and CGPLGLSLGKC; Table 1) and bsp-RGD(15) adhesion peptide (CGGNGEPRGDTYRAY) were synthesized by United BioSystem Inc (Herndon, VA). Non-degradable thiol-PEG-thiol linker (3400 kDa) was purchased from LAYSAN BIO (HUNTSVILLE, AL). Calcein was purchased from Invitrogen (Carlsbad, CA). Propium iodide, rabbit polyclonal anti-CD31 IgG, rabbit polyclonal anti-NG2 IgG, rabbit polyclonal anti-Collagen IV, and rabbit polyclonal anti-laminin were purchased from Abcam (Cambridge, MA). All chemicals were used as received. All cell culture reagents and 1× Dulbecco's phosphate buffered saline (DPBS), rhodamine labeled phalloidin were purchased from Invitrogen (Carlsbad, CA).

2.2. Synthesis of AcHyA hydrogel

HyA based hydrogels were synthesized using previously reported methods [6,7,33]. Briefly, HyA derivative carrying hydrazide groups (HyAADH) was synthesized using previously described methods [34—36], and acryloxysuccinimide (700 mg) was subsequently reacted to the HAADH solution (300 mg, 100 mL DI water) to generate acrylate groups on the HyA (AcHyA) [36—38]. Then, AcHyA-RGD derivative was synthesized by reacting CGGNGEPRGDTYRAY (bsp-RGD(15)) (10 mg) with AcHyA solution (25 mg, 10 mL DI water) at room temperature. Separately, thiolated-heparin was synthesized by reacting heparin (50 mg, 10 mL DI water) with the excess of cysteamine in the presence of EDC and HOBt at pH 6.8. AcHyA (4 mg), AcHyA-RGD (6 mg), and heparin-SH (0.03 wt%) were dissolved in 0.3 mL of TEOA buffer, then HyA hydrogels were fabricated by *in situ* crosslinking of the HyA precursors with bis-cysteine containing MMP cleavable peptides and HS-PEG-SH as a control (3 mg, 50 μL TEOA buffer) (Table 1) [6,7,25,26,33].

2.3. Cell culture, cell viability, adhesion and proliferation

Isolated GFP⁺/Sca-1⁺/CD105⁺/CD45⁻ CPCs were cultured in Iscove's Modified Dulbecco's Medium (IMDM) basal media containing 10% Fetal bovine serum (FBS) and 1% Penicillin-Streptomycin (PS) as previously described [12,20,21]. Cells were encapsulated in the hydrogels at the density of 5×10^6 cells/mL as described in our previous report [7]. Subsequently, cell viability was assessed by a Live/Dead staining kit, cell attachment was characterized by F-actin staining, and cell proliferation was quantified using the Alamar blue assay [7].

2.4. Flow cytometry

Cells entrained within the hydrogels were fixed with 4% paraformaldehyde for 30 min and permeabilized with 0.1% Triton for 5 min. After blocking with Fc-isotope controls for 10 min, the cells were stained with Allophycocyanin (APC)-conjugated anti-CD31 (PECAM-1) antibody or APC-conjugated anti-CD144 (VE-cadherin) antibody at 1:100 dilutions for 1 h in dark. The hydrogels were then degraded with 100 unit/mL hyaluronidase for 4 h to release the encapsulated cells. The stained cells were then pelleted by centrifugation, rinsed twice in PBS, passed through a 36-μm mesh cell strainer, and analyzed using a FC500 FACS Vantage cell sorter (BD Biosciences).

2.5. Immunocytochemistry

For immunocytochemistry, hydrogel samples were fixed using 4% (v/v) paraformaldehyde for 30 min and permeabilized with 0.1% Triton X-100 for 5 min. After blocking with 3% BSA for 1 h, hydrogel samples were incubated overnight at 4 °C with a 1:200 dilution of primary antibody (rabbit anti-CD31 IgG). After washing the cells 3× with PBS, hydrogel samples were incubated with a 1:200 dilution of goat anti-rabbit AlexaFluor Texas red IgG (Invitrogen, Molecular Probes) for 2 h at RT. Prior to imaging, cell nuclei were stained DAPI for 5 min at RT. Cell—gel constructs were visualized using a Prairie two photon/confocal microscope (Prairie Technologies, Middleton, WI).

2.6. MMP-2, MMP-9, MMP-13 and VEGF₁₆₅ production using ELISA

Cell/gel constructs were cultured in 400 μL cell culture media. At predetermined time points over the course of 3 weeks, the surrounding culture media and gels were collected and digested in hyaluronidase (3000 unit/mL). Subsequently, supernatants were collected after centrifugation (3000 rpm, 5 min) of the degraded hydrogels. The mass of MMPs and $VEGF_{165}$ secreted by the entrained cells in collected supernatant was determined using sandwich ELISA kits (RayBiotech, Inc., Norcross GA).

2.7. Mouse angiogenesis protein profiler array

The endogenous vascularization-associated proteins secreted by the CPCs were measured using a mouse angiogenesis protein profiler array (R&D Systems, Minneapolis, MN) following the manufacturer's instructions. The array membrane was visualized by a chemiluminescence substrate under Bio-Rad ChemiDoc XRS System. The relative expression of the angiogenesis proteins produced by the CPCs in each of the hydrogels was measured by comparing the pixel density of each chemiluminescence image.

2.8. Transduction of firefly luciferase (fLuc) into CPCs

Lentiviral vectors were packaged as previously described [39]. Briefly, third generation vectors were packaged by transient transfection of 293T cells cultured in CPC basal medium, using a calcium phosphate precipitation protocol with lentiviral transfer vector (10 μg) encoding firefly luciferase under the human ubiquitin promoter (hUb-fLuc), pMDLg/pRRE (5 μg), pRSV Rev (1.5 μg), and pcDNA IVS VSV-G (3.5 μg). Culture medium was changed 12 h post-transfection, and viral supernatant was recovered 48 h and 72 h post-transfection and filtered using a 0.45 μm filter. Viral particles were concentrated via ultracentrifugation and resuspended in PBS. CPC's were stably transduced with concentrated viral particles at a multiplicity of infection (MOI) of ~3.

2.9. In vivo implant performance assessments [7]

To detect the cell *in vivo*, CPCs were stably transducted with firefly luciferase (fLuc) into CPCs using previously reported procedure [7]. To evaluate the effect of degradation of HyA matrices on CPC survival and their ability to direct cell fate *in vivo*, a CPC/hydrogel suspension (100 μL) of firefly luciferase (fLuc) transduced CPCs (5 million cells/mL) was injected into the subcutaneous region of the anterior tibialis of syngeneic C57BL/6J mice. As a control, an equivalent concentration of CPCs suspended in PBS was injected into the subcutaneous region of the anterior tibialis of syngeneic C57BL/6J mice. *In vivo*, cell proliferation and survival was assessed at predetermined time points on the basis of the bioluminescent reporting of the cell viability of the implants (p/s). To evaluate the
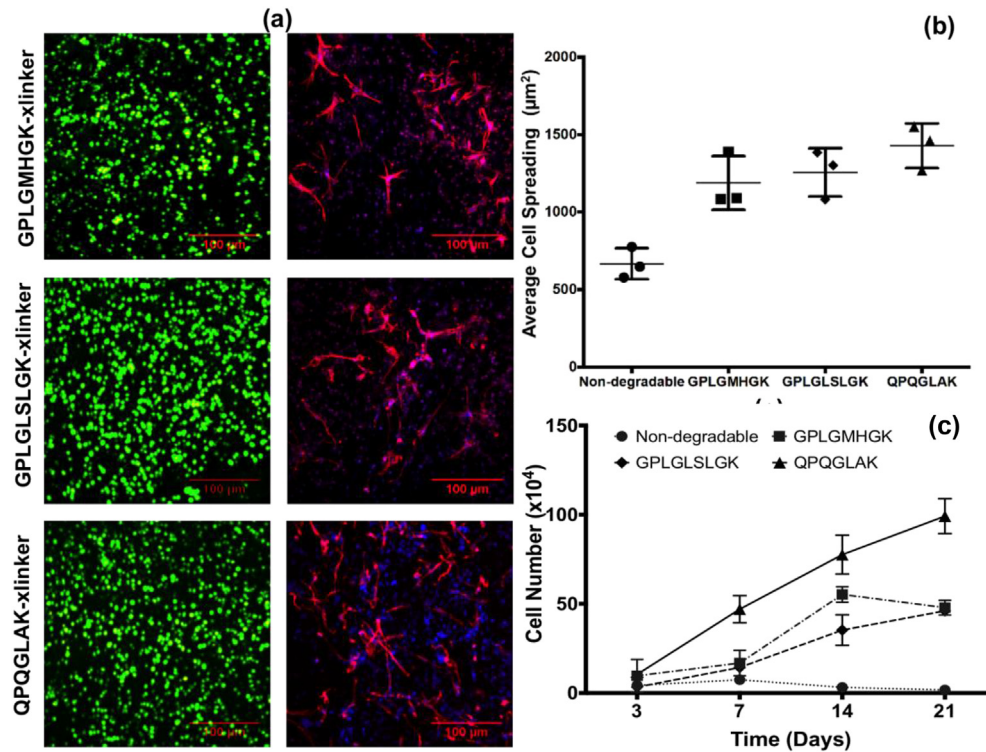
Fig. 2. CPC viability, proliferation, and adhesion in HyA hydrogels. (**a**, left panels) HyA hydrogels crosslinked by MMP cleavable peptides (GPLGMHGK, GPLGLSLGK, QPQGLAK) supported high viability of encapsulated CPCs after one day of culture, as assessed by double staining with calcein (green, live cells) and propidium iodide (red, dead cells). (**a**, right panels) CPCs were capable of adhering and spreading within all three hydrogels, as assessed by imaging of f-actin stress fibers (TRITC-phalloidin; red) and nuclei (DAPI; blue). **b**, Average spread areas of cells seeded into HyA hydrogels crosslinked with protease sensitive or insensitive (non-degradable) linkers. Average spread area of CPC in the hydrogels was calculated using Image J. **c**, Proliferation of CPCs within the HyA hydrogels was affected by type of cleavable peptide. At day 21, significantly less proliferation was seen in HyA hydrogels crosslinked with GPLGMHGK or GPLGLSLGK than with QPQGLAK; no proliferation was observed in the HyA hydrogel crosslinked by a non-degradable linker (ANOVA with Tukey, p < 0.05). (For interpretation of the references to color in this figure legend, the reader is referred to the web version of this article.)

vascular relationship of host and implant, cardiac perfusion of AF568-conjugated isolectin GS-IB4 from Griffonia simplicifolia (Invitrogen) was performed. Reconstruction of confocal images of the isolectin-perfused explants was visualized with two-photon confocal microscopy (Prairie Technologies, Middleton, WI). Matrix deposition and neovascularization was assessed in fixed (4% para-formaldehyde) and cryosectioned tissue sections.

2.10. Multiplexed bead based immunoassay

Snap frozen tissue explants were partially thawed and the protein extracted by homogenizing the tissue in cell lysis buffer, using a Bio-Plex cell lysis kit (Bio-Rad, Hercules, CA). The homogenate was centrifuged and the supernatant was collected and quantified using a DC protein assay kit (Bio-Rad, Hercules, CA). The expression of a range of angiogenesis-related factors was quantified using a Bioplex Multiplex System and a custom-designed mouse-cytokine bead-based ELISA assay, according to the manufacturer's instructions.

2.11. Statistical analysis

All quantitative measurements were performed on at least triplicate hydrogel/cell constructs. All values are expressed as means ± standard deviations (SD). One-way ANOVA with Tukey *post-hoc* tests were used to compare treatment groups in the quantitative measurements and p < 0.05 was used to assess statistical significance.

3. Results and discussion

3.1. Synthesis of HyA hydrogel

In an effort to enhance transplanted stem cell survival and improve engraftment, we recently developed a HyA-based hydrogel system, which includes a number of key material features: peptide sequences for cell attachment, heparin for sequestration/retention of exogenous/endogenous growth factors, and an enzymatically-degradable MMP-sensitive peptide as a crosslinker [7]. An optimized formulation for culturing CPCs was G′ ~ 850 Pa, 380 μM bsp-RGD (15) adhesion peptide (CGGNGEPRGDTYRAY), 0.03 wt% HMWH, 40 nM TGFβ1 [6,7]. To determine the effects of degradation kinetics of matrices on cell behavior and neovascularization *in vivo*, we synthesized gels using three protease degradable peptides that exhibit distinctly different Michaelis–Menten k_{cat}/K_m parameters (Table 1) (as a predictor of hydrogel degradation) while keeping the other matrix parameters constant as defined above [14,25].

3.2. CPC adhesion, proliferation, and differentiation are dependent on types of MMP

The effect of matrix degradation on encapsulated CPCs (Sca1^{+}/CD45^{−}) was assessed by measuring survival, proliferation, cell differentiation into the endothelial phenotype, and neovascularization [6,7]. To culture Sca-1^{+}/CD45^{−} CPCs in the HyA hydrogels, bsp-RGD (15) was chosen as a cell adhesive peptide, as we have previously shown excellent CPC adhesion and proliferation
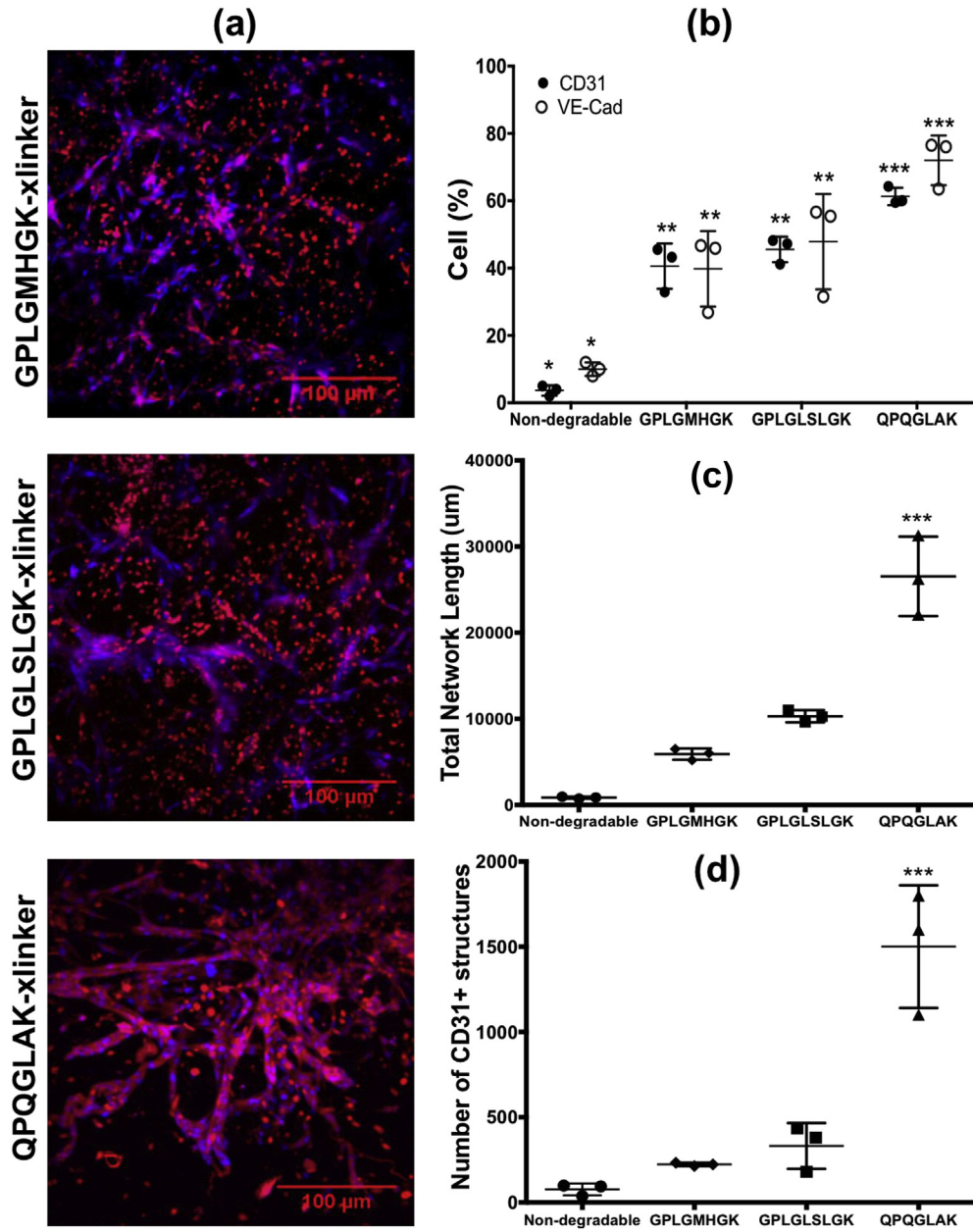
Fig. 3. Dependence of CPC differentiation and tube formation on MMP-degradable crosslinker. a, Representative confocal microscopic images of CPCs immunostained with endothelial cell marker CD31 and VE-Cad after 12 days of culture in HyA hydrogels. CPCs grown in HyA hydrogels crosslinked with the slowly degrading QPQGLAK linker exhibited significantly higher endothelial cell differentiation than CPCs grown in other hydrogels. **b**, Cell numbers quantitated by flow cytometry. **c**, Total tube network length. **d**, Total numbers of CD31+ structures. *p < 0.05.
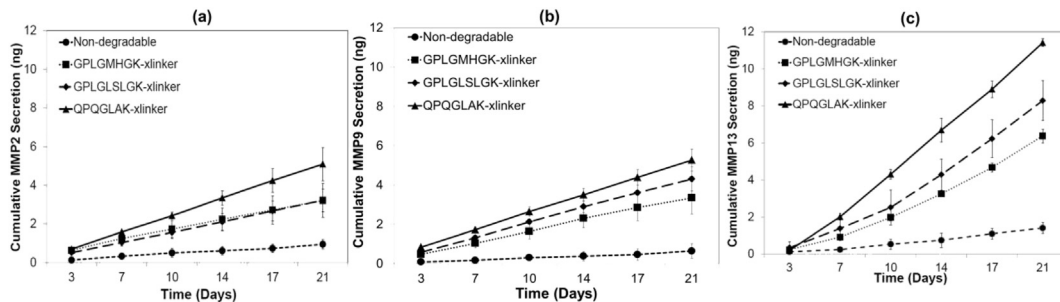
Fig. 4. Peptide crosslinkers affect matrix metalloproteinase secretion. Secretion of individual MMPs by CPCs encapsulated within HyA hydrogels during 21-day culture determined by ELISA assays specific for MMPs (a) 2, (b) 9 and (c) 13.
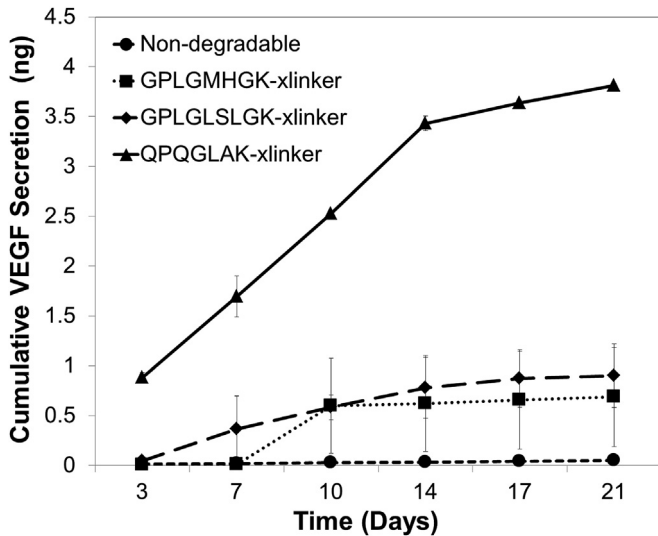
Fig. 5. HyA hydrogels promoted the secretion of VEGF$_{165}$ by CPC. VEGF$_{165}$ secreted by encapsulated CPCs was measured using VEGF$_{165}$ ELISA.

[6,7], and it also specifically interacts with several angiogenesis related receptors such as $\alpha_v\beta_3$, $\alpha_v\beta_1$, and $\alpha_5\beta_1$ [39−42]. Exogenous TGFβ1 was selected as a growth factor, since it has a heparin binding domain and it can induce CPCs to differentiate into the endothelial cells and promotes capillary tube formation [6,7,43]. HMWH was chosen for the presentation of growth factors within the HyA network as in our previous report HMWH (10.6 kDa, PDI 1.14) demonstrated better retention of TGFβ1 compared to either unfractionated (9.3 kDa, PDI 1.38) or low molecular weight heparin (4.0 kDa, PDI 1.02) [6].

Hydrogels containing protease cleavable linkages (QPQGLAK, GPLGMHGK, and GPLGLSLGK) supported the survival (>95%), robust spreading, and elongated morphology of CPCs (Fig. 2). By comparison, significant CPC death was observed in hydrogels crosslinked with the non-degradable PEG linker. Cells seeded into hydrogels crosslinked with protease sensitive linkers spread significantly more (1200−1400 μm^2, p < 0.05) than cells seeded into hydrogels crosslinked with the PEG linker (600 μm^2) (p < 0.05) (Fig. 2b) (Fig. S1). In hydrogels crosslinked with the slowly

degradable QPQGLAK linker, CPCs proliferated consistently at the highest rate among the four hydrogels (p < 0.05) (Fig. 2c). Significantly, less proliferation occurred in gels crosslinked with the more rapidly degradable peptides GPLGMHGK and GPLGLSLGK. No proliferation of CPCs was observed in the hydrogels crosslinked with the non-degradable linker (Fig. 2c). This can be attributed to the inability of the cells to remodel the matrix, thus constraining their capacity to expand.

Differentiation of CPCs into endothelial cells (ECs) within the hydrogels was assessed by immunostaining for the endothelial cell surface marker CD31, tubule quantification was performed on z-stacked confocal images of CD31 staining using FIJI (National Institutes of Health, Bethesda, MD), and quantifying by flow cytometry for the EC-specific markers CD31 and VE-Cadherin (VECAD) (Fig. 3). Endothelial differentiation and tube formation depended on matrix degradation kinetics. The dense vascular network formation correlated with increased expression of EC markers CD31 and VECAD (Fig. 3b) (p < 0.05), and the highest total tube length and number of tubes were observed, in the HyA hydrogel crosslinked with the QPQGLAK peptide compared to the more rapidly degradable peptides GPLGMHGK and GPLGLSLGK (Fig. 3c, d). However, even with the same presentation of TGFβ1 in the non-degradable hydrogel, CPCs did not appreciably differentiate into endothelial cells, and therefore did not form tubular networks (Fig. 3b−c; Fig. S1).

In all the MMP-degradable HyA hydrogels, CPCs differentially expressed MMP-2, -9, and -13 (Fig. 4). It has been previously shown that TGFβ1 induces endothelial cell expression of MMP-2, MMP-9, and MMP-13 [44−46], which, in this study, resulted in degradation of each matrix consistent with their degradation kinetics as per their Michaelis−Menten k_{cat}/K_m parameters (Table 1). Interestingly, compared to HyA hydrogels crosslinked with the rapidly degrading peptides, GPLGMHGK and GPLGLSLGK, the highest levels of MMP-2, -9, and -13 were secreted in the HyA hydrogel crosslinked with slowly degrading (lowest k_{cat}/K_m) peptide, QPQGLAK. Additionally, compared to MMP-2 and -9, MMP-13 was secreted in highest amount by entrained CPCs independent of peptide crosslinker used (Fig. 4). Since the major difference in enzyme kinetics (i.e., k_{cat}/K_m) between the various peptide crosslinkers occurs with MMP-13 (Table 1), we suggest in our system that matrix degradation is dominated by MMP-13. The generality of this observation is premature and needs further study with additional cell types.
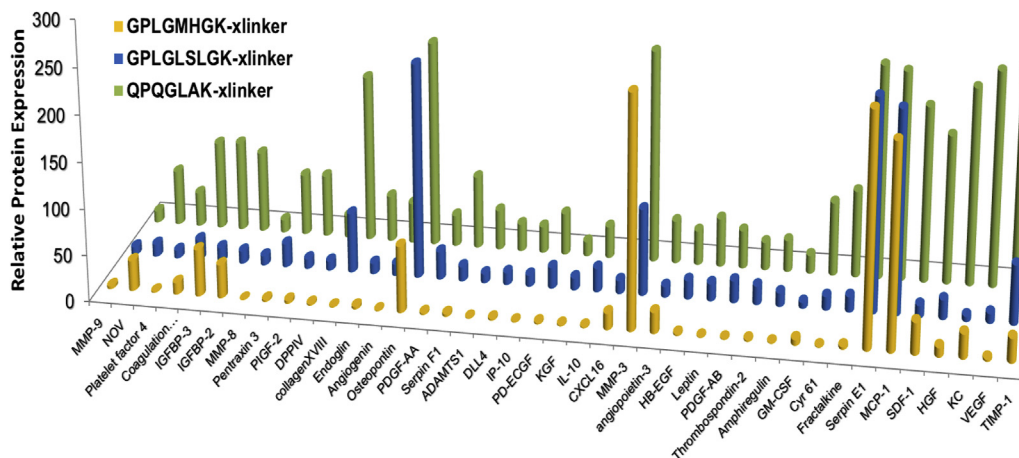
Fig. 6. Angiogenic cytokine expression by CPCs. The relative expression of secreted angiogenic factors produced by CPCs and sequestered within HyA hydrogel after 12 days as determined by mouse angiogenesis protein profiler array (R&D Systems, Minneapolis, MN). Relative expression of secreted proteins was determined by quantifying the mean spot pixel density from the arrays using image software analysis (Image J Software). Production of angiogenesis proteins in HyA hydrogel was dependent on degradation kinetic of MMP cleavable crosslinkers.
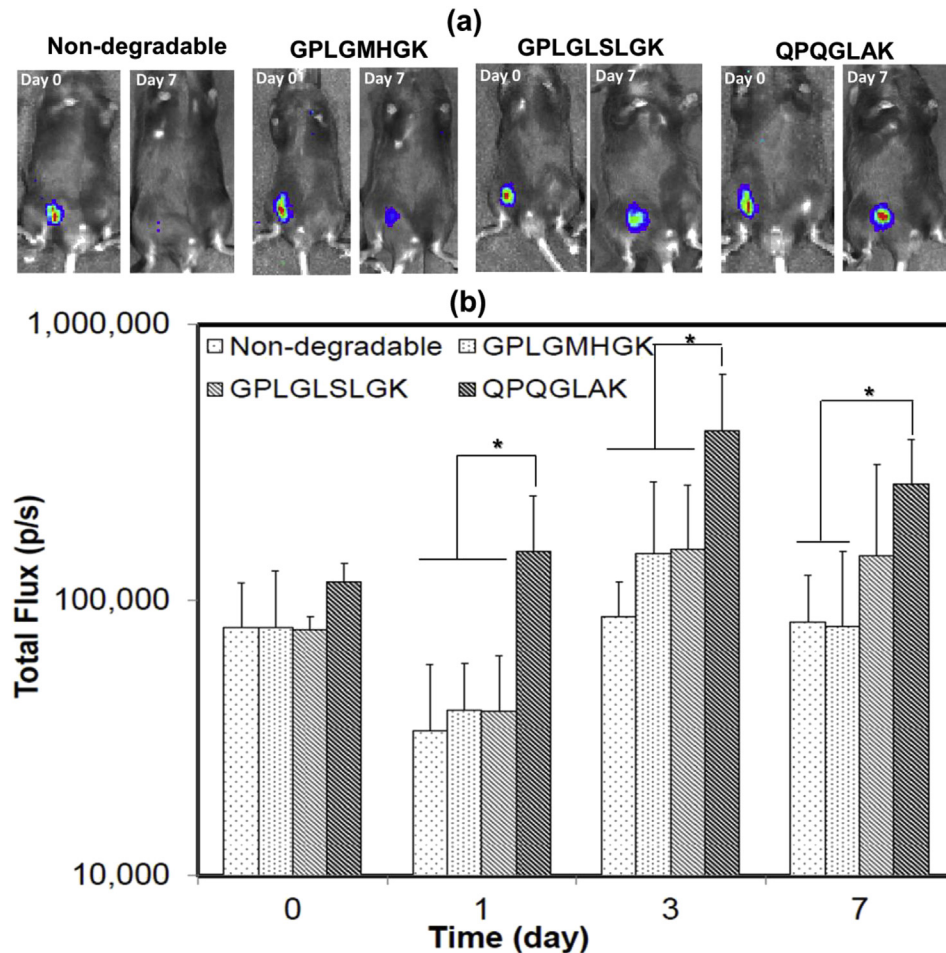
Fig. 7. HyA hydrogels promoted CPC survival. To confirm the *in vivo* survival of CPCs, **a**. Bioluminescence was observed post-implantation of (~500,000 cells in 100 μL gel) in syngeneic mouse hindlimb using HyA hydrogel. **b**, Total radiance (p/s) generated by the transplanted CPCs demonstrated that CPCs proliferated modestly in all the hydrogels after day 1, with the greatest number of cells in the QPQGLAK and GPLGLSLGK crosslinked hydrogels by day 7.

Previous studies have identified MMP-13 expression as a critical factor that directly contributes to the process of neovascularization. For example, MMP-13 deficient mice have been shown to have impaired angiogenesis and delayed repair of bone fracture [47–49]. In another study, conditioned medium from MMP-13-overexpressing cells stimulated capillary formation of immortalized human umbilical vein endothelial cells (HUVECs), while treatment of HUVECs with recombinant MMP-13 protein enhanced capillary tube formation both *in vitro* and *in vivo* [50]. Furthermore, production of MMP13 induces the secretion of VEGF from fibroblasts and endothelial cells, and promotes angiogenesis by activation of FAK and ERK pathways [20,49–51]. Consistent with these previous reports, we observed that the high amount of MMP-13 retained in the QPQGLAK-linked hydrogel induced significantly higher amounts of $VEGF_{165}$ compared to rapidly degradable GPLGMHGK- and GPLGLSLGK-linked hydrogels (Fig. 5). In spite of having identical features as the peptide crosslinked hydrogels (i.e., adhesion peptides and exogenous TGFβ1), negligible amounts of MMP-2, -9, -13 and $VEGF_{165}$ were produced in the non-degradable HyA hydrogel (Figs. 4 and 5). Clearly, CPCs have sensitive matrix requirements for optimal performance.

$VEGF_{165}$ is a major signaling protein involved in promoting the proliferation and differentiation of the endothelial lineage from the earliest stages of angiogenesis by the association of produced $VEGF_{165}$ with VEGFR-2 on endothelial cells [52–55]. Thereby, the highest $VEGF_{165}$ expression in the slowly degradable QPQGLAK crosslinked HyA hydrogel resulted in the highest endothelial differentiation as confirmed by the highest expression of $CD31^+$ and $VECAD^+$ endothelial cells, which then produced a dense vascular-like network (Fig. 3). Covalently linked HMWH in HyA hydrogel has been shown to have the capacity to sequester multiple endogenously secreted angiogenic factors within the matrix, and subsequently support the trophic functions of the CPCs [6]. Therefore, we assessed the effect of matrix degradation on sequestering capacity of hydrogels. Similar to other results, the slowly degradable QPQGLAK peptide in HyA hydrogels exhibited significantly higher retention and presentation of a wide array of angiogenic proteins in the matrices secreted by the entrained CPCs relative to fast degradable peptides GPLGMHGK, and GPLGLSLGK, which enabled a prolonged bioactive effect on the entrained CPCs (see Fig. 6, Fig. S4).

3.3. In vivo performance of selective MMP degradable crosslinkers

To assess the effect of matrix degradation on cell survival, differentiation, and engraftment *in vivo*, cell-laden hydrogels were injected in a subcutaneous region of syngeneic C57BL/6 mice hindlimbs, and the bioluminescent signal (p/s) of the implant sites was monitored. Within one day of transplantation all the hydrogels had significant cell death, except the one crosslinked with QPQGLAK
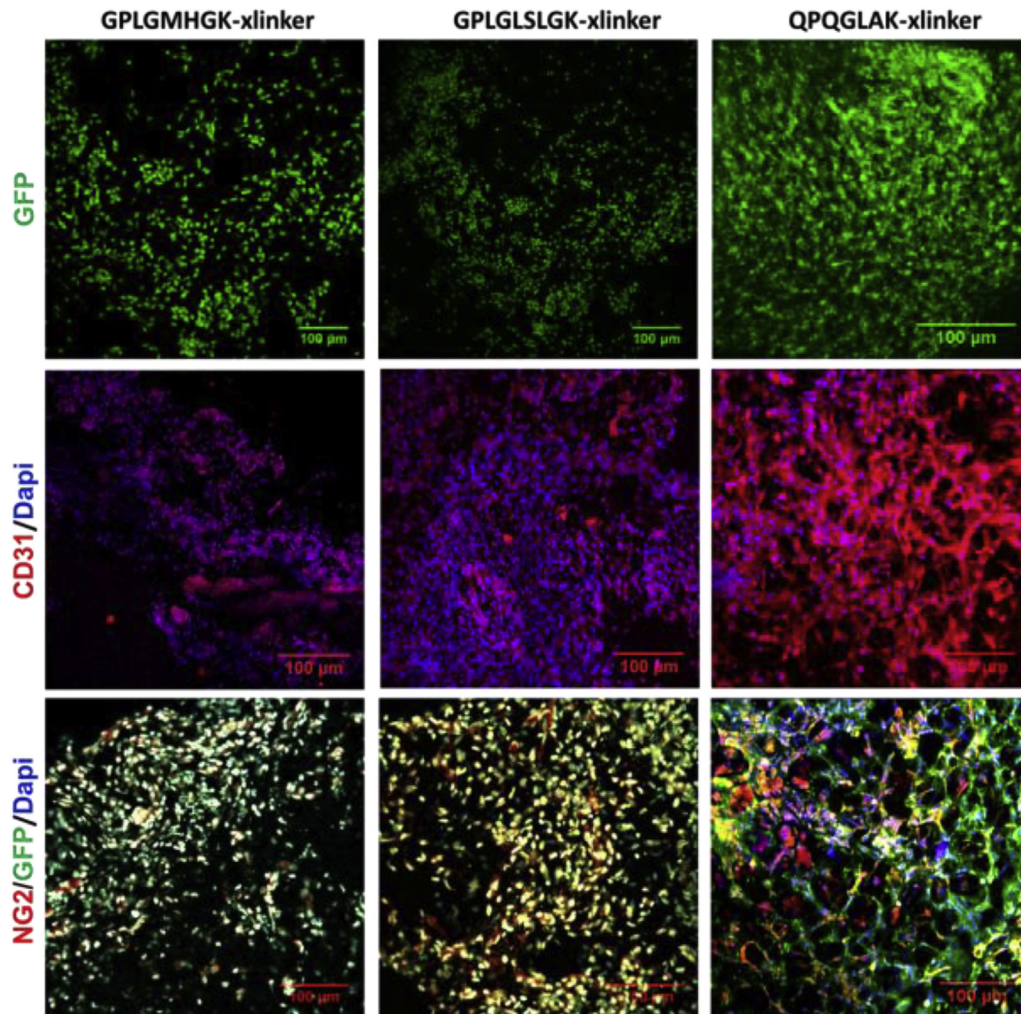
Fig. 8. *In vivo* **CPC survival, differentiation and infiltration of pericyte cells**. Verification of the persistence of donor CPCs with GFP expression, and differentiation of CPCs into endothelial cells was confirmed by expression of CD31. HyA hydrogel formed by slowly degradable peptide fostered significant and mature blood vessel formation, and infiltration of NG2$^+$ pericytes was observed alongside the donor GFP$^+$ cells. Scale bars = 100 μm.

(Fig. 7) (p < 0.05). CPCs proliferated modestly in all the hydrogels after day 1, with the greatest number of cells in the QPQGLAK and GPLGLSLGK crosslinked hydrogels by day 7 (p < 0.05). We anticipate that rapid vascularization and slow degradation of QPQGLAK supported the highest cell survival in these matrices, whereas rapid degradation of other matrices led to reduced mechanical support for the cells, which translated into altered profiles of secreted angiogenic proteins, and subsequently reduced vascular networks and angiogenesis *in vivo*. However, in contrast, the non-degradable PEG group had significantly lower vascularization due to the lack of cell-mediated matrix remodeling. It is noteworthy that, at sacrifice (day 7), tissue-like intact matrix was observed at the site of slowly degradable QPQGLAK hydrogel; however, faster degrading GPLGMHGK and GPLGLSLGK hydrogels were disintegrated into small chunks. In contrast, at the injection site of the PEG crosslinked hydrogel, a thick mass of hydrogel was observed due to minimal degradation of PEG crosslinked matrices.

Explants were cryosectioned and stained to identify cell types and ECM present within the hydrogel. Confocal images of the implants exhibited a higher density of GFP$^+$ donor cells in QPQGLAK hydrogel compared to either GPLGMHGK or GPLGLSLGK crosslinked gels (Fig. 8). CD31 staining demonstrated the presence of CD31$^+$ cells and a vascular-like network throughout the QPQGLAK

implant. Interestingly, NG2$^+$ pericytes had infiltrated the QPQGLAK implants and were observed surrounding the GFP$^+$ donor cells (Fig. 8; Fig. S6). In contrast, an insignificant number of CD31$^+$ and NG2$^+$ cells were observed in fast degradable (GPLGMHGK, and GPLGLSLGK) and non-degradable hydrogels (Fig. 8; Fig. S2). Furthermore, Masson's trichrome staining indicated a collagen mesh-like network as shown in blue throughout the QPQGLAK explants; in contrast, cells in GPLGMHGK, GPLGLSLGK, and non-degradable crosslinked hydrogels contained minimal collagen and lacked structure (Fig. 9; Fig. S2). Furthermore, cells in the QPQGLAK crosslinked hydrogels induced the secretion of the greatest amount of basement membrane matrix containing Type IV collagen and laminin, which were uniformly distributed throughout the implants. Some hydrogel was shed from the GPLGMHGK, and GPLGLSLGK specimens during tissue processing and cryosectioning as a result of their rapid degradation and the low amount of matrix formation supported by these materials. In order to confirm cell infiltration from host tissue and matrix production by these cells in the implants, we also performed Trichrome Masson's staining on acellular implants (Fig. S5), which confirmed that majority of matrix was produced by donor cells. Collectively, these observations indicated that the slower degrading matrix ($k_{cat}/K_m = 7.5 \times 10^2$ s^{-1} M^{-1}), allowed for balanced production of ECM
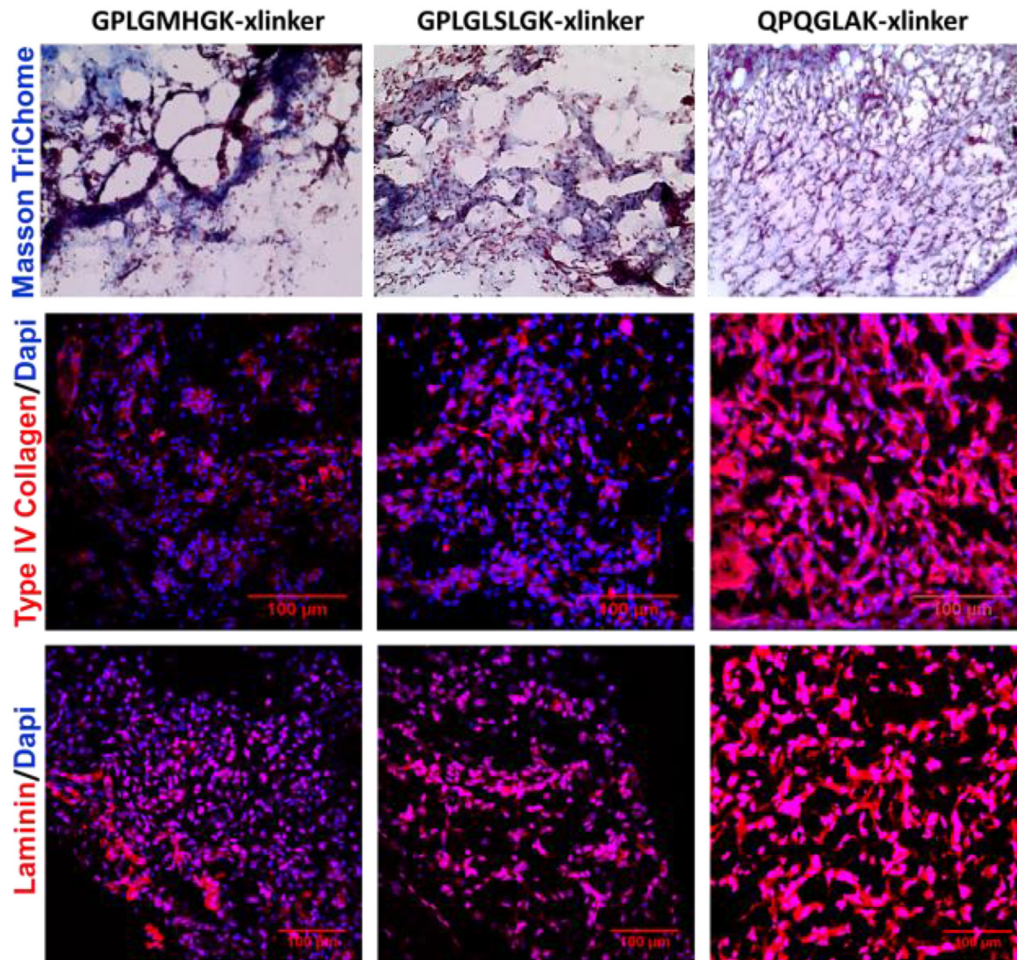
Fig. 9. Extracellular matrix production by histology. The QPQGLAK explants exhibited strong collagen staining by Masson's trichrome, which was rich with Type IV collagen and laminin, as visualized by immunohistochemistry. Scale bars = 100 μm.

proteins that supported CPC differentiation into endothelial cells.

To evaluate angiogenesis and the integration of vessels within the implant with the host's, newly formed blood vessels in the implants were immunostained for endomucin and by systemic cardiac perfusion of the Alexa Fluor 568-conjugated GS-IB4 lectin through the host blood circulation. Complex vascular structures were observed in the explants by reconstruction of confocal images of isolectin, which clearly indicated the vessels within the QPQGLAK crosslinked hydrogel were anastomosed with the host vessels (Fig. 10; Fig. S7). Vascular structures were clearly visible in QPQGLAK explants with cross sectional areas ranging from 100 to 30,000 μm^2. Negligible vasculature could be discerned in the other hydrogels including the non-degradable hydrogel after perfusion of AF-568 GS-IB4 lectin or endomucin staining (Fig. 10 and Fig. S3).

We analyzed the angiogenic protein production of the explanted hydrogels by multiplex ELISA at day 1 and at sacrifice (day 7) (Fig. 11). At day 1, QPQGLAK hydrogels stimulated the highest expression of VEGF, FGF, KC and IL-6 when compared with other hydrogels. At day 7, expression of these proteins was down-regulated in QPQGLAK implants, whereas these proteins were upregulated for both the GPLGMHGK, and GPLGLSLGK implants (Fig. 11). Non-degradable implants exhibited the lowest expression of all of these proteins except $VEGF_{165}$. We suggest that the higher expression of $VEGF_{165}$, FGF, KC and IL-6 at day 1 in QPQGLAK hydrogels promoted angiogenesis and maturation of newly formed vessels within implants that we observed by day 7 (Fig. 10). We

attribute the excellent cell survival in QPQGLAK crosslinked implants to this rapid vessel development within the implant. At day 7, NG2$^+$ cells were observed throughout the QPQGLAK implant (Fig. 8). We suspect that interaction of NG2$^+$ pericytes and CD31$^+$ endothelial cells induces the maturation of new-formed vessels. In this regard, interactions between pericytes and endothelial cells are known to support vessel maturation and stabilization by secretion of TIMPS [56—59]. It has also been shown that angiogenesis and invasion in 3D collagen matrices occurs within 48 h and is accompanied by the degradation of the surrounding matrix. Subsequent endothelial—pericyte interactions induce TIMP secretion, which reduces the MMP activity of endothelial cells resulting in reduced degradation of the surrounding matrix and a reduction in secretion of angiogenic proteins, leading to the maturation of newly formed vessels [58]. To confirm these results in our system, we determined the level of MMP-2, MMP-9, and MMP-13 in the hydrogel explants using ELISA at day 1 and day 7. Level of MMP-2, MMP-9, and MMP-13 was higher at day 1 and lower at day 7 in QPQGLAK hydrogels (Fig. S8). In contrast with QPQGLAK implants, angiogenic proteins and level of MMPs in GPLGMHGK, and GPLGLSLGK implants were upregulated at day 7 (Fig. 11). It is noteworthy that, by day 7, GPLGMHGK and GPLGLSLGK crosslinked hydrogels were already fragmenting; therefore, it is possible that the production of angiogenic proteins analyzed by multiplex ELISA was, in part, due to production occurring in tissues surrounding the injection site of the GPLGMHGK and GPLGLSLGK hydrogels.
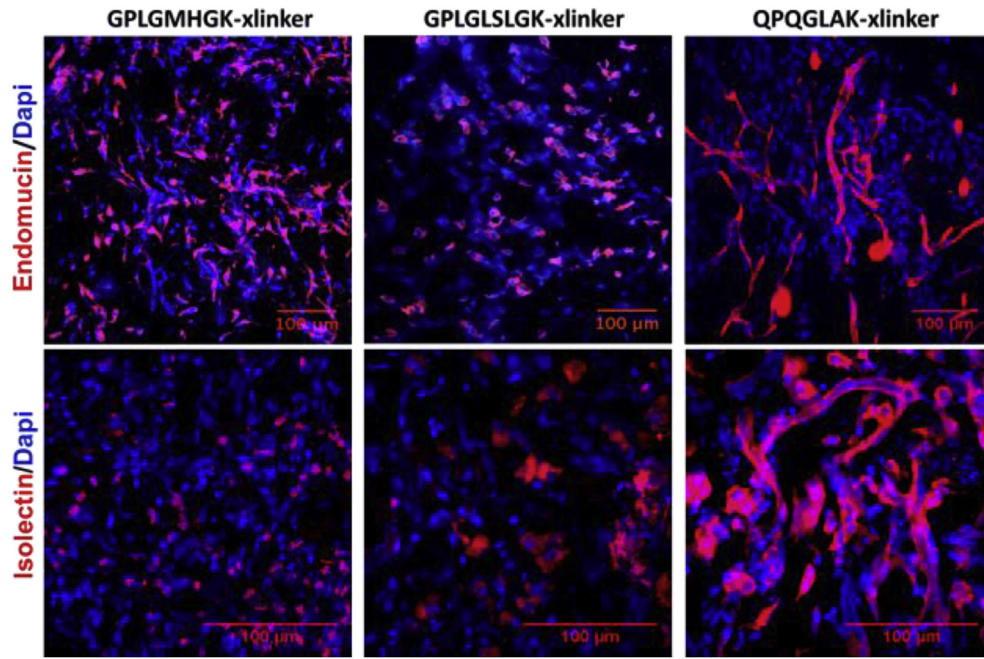
Fig. 10. Assessment of vascular tone development in HyA hydrogel. Vascular tone in the explants was evaluated by endomucin staining, and integration of the hydrogels with the host vasculature was assessed by systemic perfusion of the host with Alexa Fluor 568-conjugated GS-IB4 lectin (isolectin). Reconstruction of confocal images of endomucin staining and isolectin perfusion clearly indicates that vessels within the HyA hydrogels only crosslinked by QPQGLAK were anastomosed with the host vessels. Scale bars = 100 μm.
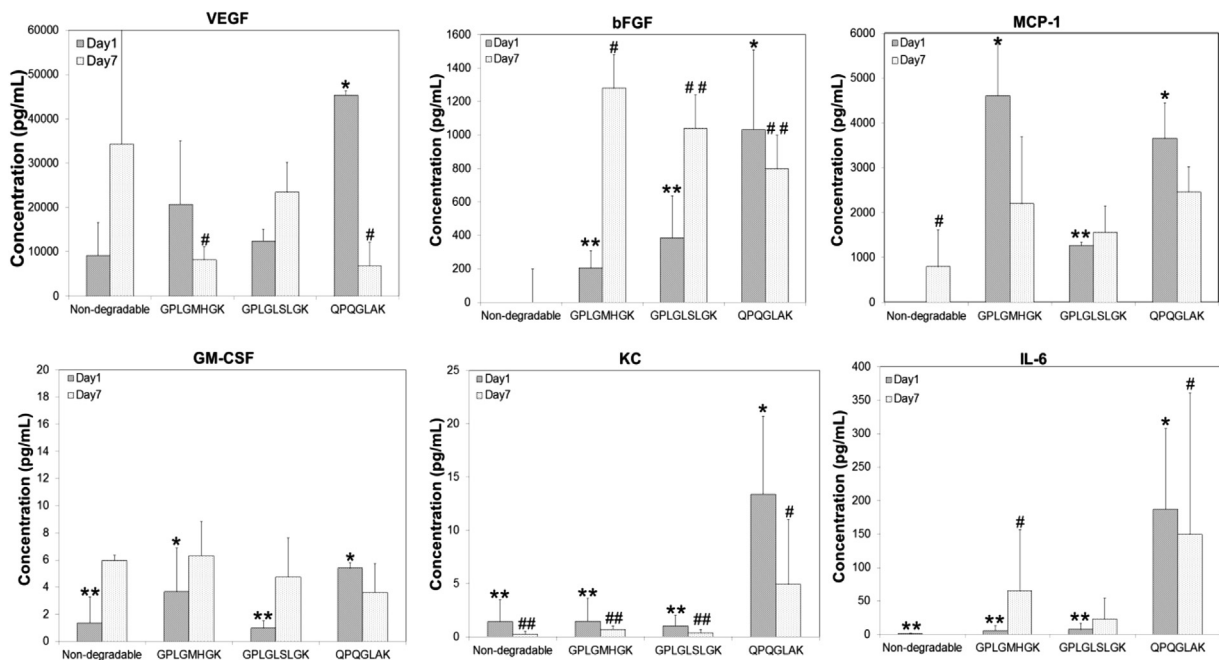
Fig. 11. *In vivo* secreted proteins. At day 1, QPQGLAK hydrogels stimulated highest expression of $VEGF_{165}$, FGF, KC and IL-6 compare to other hydrogels; however, at day 7 these proteins were upregulated for GPLGMHGK, and GPLGLSLGK implants day 7. Non-degradable implants had the lowest expression of all of these proteins except the $VEGF_{165}$. These results demonstrate that process of vascularization was started at day 1 and stabilized at day 7 for QPQGLAK implant.

Overall, the slowly degrading QPQGLAK crosslinked hydrogel enhanced the functional impact of donor cell transplantation via robust engraftment and timely vasculature development in the implant. Specifically, the transplanted CPCs in the QPQGLAK hydrogels differentiated into blood vessel phenotypes and formed new blood vessels that anastomosed with the host's circulatory system. *In vitro* data clearly demonstrated that QPQGLAK hydrogels

supported the highest production and prolonged retention of MMP-13, $VEGF_{165}$, and various angiogenesis related proteins (see, Figs. 4–6) which stimulated rapid vessel-like networks. *In vivo* all of these factors supported the survival and engraftment of CPCs and their progeny, and stimulated the processes of angiogenesis and anastomosis with the host's circulatory system. It is worth mentioning that this preliminary validation of our HyA hydrogel

system is carried out in a subcutaneous model. We note the caveat that the subcutaneous model is very simplified and has less MMP-activity and inflammation in the microenvironment compared to an ischemic injury model. Thus, in future studies, we will assess this system in an ischemic injury model, with the potential to further optimize the MMP-mediated degradation and taking into account the altered microenvironment.

4. Conclusions

HyA hydrogels crosslinked the MMP-degradable peptide QPQGLAK supports the greatest CPC survival, proliferation, and endothelial cell differentiation compared to the other crosslinkers tested. These QPQGLAK crosslinked hydrogels induced the highest amount of production of MMP2, MMP9, MMP13, VEGF$_{165}$, and angiogenesis related proteins. They also supported the prolonged retention of these proteins that further stimulated rapid vascular development within implanted constructs that anastomosed with the host circulatory system. Synthetic matrices formed by cross-linking with MMP-13 degradable peptides with a k_{cat}/K_m in the range of ~10^2 allows for controlled remodeling of matrices, leading to improved cellular functions and better engraftment of trans-planted CPCs. Collectively, the results of this study demonstrate the significance of crosslinker degradation kinetics on stem cell function and engraftment of donor stem cells.

Acknowledgments

Appendix A. Supplementary data

Supplementary data related to this article can be found at http://dx.doi.org/10.1016/j.biomaterials.2016.02.023.

References

[1] H. Liu, Y. Kim, S. Sharkis, L. Marchionni, Y.Y. Jang, In vivo liver regeneration potential of human induced pluripotent stem cells from diverse origins, Sci. Transl. Med. 3 (2011) 82ra39.

[2] K. Matsuura, A. Honda, T. Nagai, N. Fukushima, K. Iwanaga, M. Tokunaga, et al., Transplantation of cardiac progenitor cells ameliorates cardiac dysfunction after myocardial infarction in mice, J. Clin. Investig. 119 (2009) 2204—2217.

[3] J.Y. Min, M.F. Sullivan, Y. Yang, J.P. Zhang, K.L. Converso, J.P. Morgan, et al., Significant improvement of heart function by cotransplantation of human mesenchymal stem cells and fetal cardiomyocytes in postinfarcted pigs, Ann. Thorac. Surg. 74 (2002) 1568—1575.

[4] Y. Mizuno, H. Chang, K. Umeda, A. Niwa, T. Iwasa, T. Awaya, et al., Generation of skeletal muscle stem/progenitor cells from murine induced pluripotent stem cells, FASEB J. 24 (2010) 2245—2253.

[5] J.V. Terrovitis, R.R. Smith, E. Marban, Assessment and optimization of cell engraftment after transplantation into the heart, Circ. Res. 106 (2010) 479—494.

[6] A.K. Jha, A. Mathur, F.L. Svedlund, J. Ye, Y. Yeghiazarians, K.E. Healy, Molecular weight and concentration of heparin in hyaluronic acid-based matrices modulates growth factor retention kinetics and stem cell fate, J. Control.

[7] Release — Off. J. Control. Release Soc. 209 (2015) 308—316.

[7] A.K. Jha, K.M. Tharp, J. Ye, J.L. Santiago-Ortiz, W.M. Jackson, A. Stahl, et al., Enhanced survival and engraftment of transplanted stem cells using growth factor sequestering hydrogels, Biomaterials 47 (2015) 1—12.

[8] S.J. Bryant, K.L. Durand, K.S. Anseth, Manipulations in hydrogel chemistry control photoencapsulated chondrocyte behavior and their extracellular matrix production, J. Biomed. Mater. Res. A 67 (2003) 1430—1436.

[9] J.P. Jain, S. Modi, N. Kumar, Hydroxy fatty acid based polyanhydride as drug delivery system: synthesis, characterization, in vitro degradation, drug release, and biocompatibility, J. Biomed. Mater. Res. A 84 (2008) 740—752.

[10] D.S. Benoit, A.R. Durney, K.S. Anseth, Manipulations in hydrogel degradation behavior enhance osteoblast function and mineralized tissue formation, Tissue Eng. 12 (2006) 1663—1673.

[11] X. Guo, H. Park, G. Liu, W. Liu, Y. Cao, Y. Tabata, et al., In vitro generation of an osteochondral construct using injectable hydrogel composites encapsulating rabbit marrow mesenchymal stem cells, Biomaterials 30 (2009) 2741—2752.

[12] J.S. Temenoff, H. Park, E. Jabbari, T.L. Sheffield, R.G. LeBaron, C.G. Ambrose, et al., In vitro osteogenic differentiation of marrow stromal cells encapsulated in biodegradable hydrogels, J. Biomed. Mater. Res. A 70 (2004) 235—244.

[13] D.A. Wang, C.G. Williams, F. Yang, N. Cher, H. Lee, J.H. Elisseeff, Bioresponsive phosphoester hydrogels for bone tissue engineering, Tissue Eng. 11 (2005) 201—213.

[14] M.P. Lutolf, J.L. Lauer-Fields, H.G. Schmoekel, A.T. Metters, F.E. Weber, G.B. Fields, et al., Synthetic matrix metalloproteinase-sensitive hydrogels for the conduction of tissue regeneration: engineering cell-invasion characteristics, Proc. Natl. Acad. Sci. U. S. A. 100 (2003) 5413—5418.

[15] S. Kim, K.E. Healy, Synthesis and characterization of injectable poly(N-isopropylacrylamide-co-acrylic acid) hydrogels with proteolytically degradable cross-links, Biomacromolecules 4 (2003) 1214—1223.

[16] S. Kim, E.H. Chung, M. Gilbert, K.E. Healy, Synthetic MMP-13 degradable ECMs based on poly(N-isopropylacrylamide-co-acrylic acid) semi-interpenetrating polymer networks. I. Degradation and cell migration, J. Biomed. Mater. Res. A 75 (2005) 73—88.

[17] J. Lam, W.E. Lowry, S.T. Carmichael, T. Segura, Delivery of iPS-NPCs to the stroke cavity within a hyaluronic acid matrix promotes the differentiation of transplanted cells, Adv. Funct. Mater. 24 (2014) 7053—7062.

[18] Y. Lei, S. Gojgini, J. Lam, T. Segura, The spreading, migration and proliferation of mouse mesenchymal stem cells cultured inside hyaluronic acid hydrogels, Biomaterials 32 (2011) 39—47.

[19] Q. Feng, M. Zhu, K. Wei, L. Bian, Cell-mediated degradation regulates human mesenchymal stem cell chondrogenesis and hypertrophy in MMP-sensitive hyaluronic acid hydrogels, PLoS One 9 (2014) e99587.

[20] K.B. Fonseca, F.R. Maia, F.A. Cruz, D. Andrade, M.A. Juliano, P.L. Granja, et al., Enzymatic, physicochemical and biological properties of MMP-sensitive alginate hydrogels, Soft Matter 9 (2013) 3283—3292.

[21] Y. Park, M.P. Lutolf, J.A. Hubbell, E.B. Hunziker, M. Wong, Bovine primary chondrocyte culture in synthetic matrix metalloproteinase-sensitive poly(-ethylene glycol)-based hydrogels as a scaffold for cartilage repair, Tissue Eng. 10 (2004) 515—522.

[22] J. Patterson, J.A. Hubbell, Enhanced proteolytic degradation of molecularly engineered PEG hydrogels in response to MMP-1 and MMP-2, Biomaterials 31 (2010) 7836—7845.

[23] J. Patterson, J.A. Hubbell, SPARC-derived protease substrates to enhance the plasmin sensitivity of molecularly engineered PEG hydrogels, Biomaterials 32 (2011) 1301—1310.

[24] M.V. Turturro, M.C. Christenson, J.C. Larson, D.A. Young, E.M. Brey, G. Papavasiliou, MMP-sensitive PEG diacrylate hydrogels with spatial variations in matrix properties stimulate directional vascular sprout formation, PLoS One 8 (2013) e58897.

[25] S.T. Wall, C.C. Yeh, R.Y. Tu, M.J. Mann, K.E. Healy, Biomimetic matrices for myocardial stabilization and stem cell transplantation, J. Biomed. Mater. Res. A 95 (2010) 1055—1066.

[26] E.H. Chung, M. Gilbert, A.S. Virdi, K. Sena, D.R. Sumner, K.E. Healy, Biomimetic artificial ECMs stimulate bone regeneration, J. Biomed. Mater. Res. A 79 (2006) 815—826.

[27] S. Khetan, J.S. Katz, J.A. Burdick, Sequential crosslinking to control cellular spreading in 3-dimensional hydrogels, Soft Matter 5 (2009) 1601—1606.

[28] J. Kim, I.S. Kim, T.H. Cho, H.C. Kim, S.J. Yoon, J. Choi, et al., In vivo evaluation of MMP sensitive high-molecular weight HA-based hydrogels for bone tissue engineering, J. Biomed. Mater. Res. A 95 (2010) 673—681.

[29] L. Lin, R.E. Marchant, J. Zhu, K. Kottke-Marchant, Extracellular matrix-mimetic poly(ethylene glycol) hydrogels engineered to regulate smooth muscle cell proliferation in 3-D, Acta Biomater. 10 (2014) 5106—5115.

[30] I.L. Isa, A. Srivastava, D. Tiernan, P. Owens, P. Rooney, P. Dockery, et al., Hyaluronic acid based hydrogels attenuate inflammatory receptors and neurotrophins in interleukin-1beta induced inflammation model of nucleus pulposus cells, Biomacromolecules 16 (2015) 1714—1725.

[31] P. Rooney, A. Srivastava, L. Watson, L.R. Quinlan, A. Pandit, Hyaluronic acid decreases IL-6 and IL-8 secretion and permeability in an inflammatory model of interstitial cystitis, Acta Biomater. 19 (2015) 66—75.

[32] J. Ye, A. Boyle, H. Shih, R.E. Sievers, Y. Zhang, M. Prasad, et al., Sca-1+ cardiosphere-derived cells are enriched for Isl1-expressing cardiac precursors and improve cardiac function after myocardial injury, PLoS One 7 (2012) e30329.

[33] K.M. Tharp, A.K. Jha, J. Kraiczy, A. Yesian, G. Karateev, R. Sinisi, et al., Matrix

assisted transplantation of functional beige adipose tissue, Diabetes 64 (11) (2015) 3713–3724.

[34] A.J. Farran, S.S. Teller, A.K. Jha, T. Jiao, R.A. Hule, R.J. Clifton, et al., Effects of matrix composition, microstructure, and viscoelasticity on the behaviors of vocal fold fibroblasts cultured in three-dimensional hydrogel networks, Tissue Eng. A 16 (2010) 1247–1261.

[35] L.A. Gurski, A.K. Jha, C. Zhang, X. Jia, M.C. Farach-Carson, Hyaluronic acid-based hydrogels as 3D matrices for in vitro evaluation of chemotherapeutic drugs using poorly adherent prostate cancer cells, Biomaterials 30 (2009) 6076–6085.

[36] A.K. Jha, R.A. Hule, T. Jiao, S.S. Teller, R.J. Clifton, R.L. Duncan, et al., Structural analysis and mechanical characterization of hyaluronic acid-based doubly cross-linked networks, Macromolecules 42 (2009) 537–546.

[37] J. Kim, I.S. Kim, T.H. Cho, K.B. Lee, S.J. Hwang, G. Tae, et al., Bone regeneration using hyaluronic acid-based hydrogel with bone morphogenic protein-2 and human mesenchymal stem cells, Biomaterials 28 (2007) 1830–1837.

[38] T. Pouyani, G.D. Prestwich, Functionalized derivatives of hyaluronic acid oligosaccharides: drug carriers and novel biomaterials, Bioconjug. Chem. 5 (1994) 339–347.

[39] T.D. Arnold, G.M. Ferrero, H. Qiu, I.T. Phan, R.J. Akhurst, E.J. Huang, et al., Defective retinal vascular endothelial cell development as a consequence of impaired integrin alphaVbeta8-mediated activation of transforming growth factor-beta, J. Neurosci. 32 (2012) 1197–1206.

[40] D. Veron, G. Villegas, P.K. Aggarwal, C. Bertuccio, J. Jimenez, H. Velazquez, et al., Acute podocyte vascular endothelial growth factor (VEGF-A) knockdown disrupts alphaVbeta3 integrin signaling in the glomerulus, PLoS One 7 (2012) e40589.

[41] Z.Z. Zeng, H. Yao, E.D. Staszewski, K.F. Rockwood, S.M. Markwart, K.S. Fay, et al., alpha(5)beta(1) Integrin ligand PHSRN induces invasion and alpha(5) mRNA in endothelial cells to stimulate angiogenesis, Transl. Oncol. 2 (2009) 8–20.

[42] B.P. Eliceiri, D.A. Cheresh, The role of alphav integrins during angiogenesis: insights into potential mechanisms of action and clinical development, J. Clin. Investig. 103 (1999) 1227–1230.

[43] M.J. Goumans, T.P. de Boer, A.M. Smits, L.W. van Laake, P. van Vliet, C.H. Metz, et al., TGF-beta1 induces efficient differentiation of human cardiomyocyte progenitor cells into functional cardiomyocytes in vitro, Stem Cell Res. 1 (2007) 138–149.

[44] M.A. Behzadian, X.L. Wang, L.J. Windsor, N. Ghaly, R.B. Caldwell, TGF-beta increases retinal endothelial cell permeability by increasing MMP-9: possible role of glial cells in endothelial barrier function, Investig. Ophthalmol. Vis. Sci. 42 (2001) 853–859.

[45] R.C. Fares, A. Gomes Jde, L.R. Garzoni, M.C. Waghabi, R.M. Saraiva, N.I. Medeiros, et al., Matrix metalloproteinases 2 and 9 are differentially expressed in patients with indeterminate and cardiac clinical forms of Chagas disease, Infect. Immun. 81 (2013) 3600–3608.

[46] H.S. Kim, T. Shang, Z. Chen, S.C. Pflugfelder, D.Q. Li, TGF-beta1 stimulates production of gelatinase (MMP-9), collagenases (MMP-1, -13) and stromely-sins (MMP-3, -10, -11) by human corneal epithelial cells, Exp. Eye Res. 79 (2004) 263–274.

[47] N. Kosaki, H. Takaishi, S. Kamekura, T. Kimura, Y. Okada, L. Minqi, et al., Impaired bone fracture healing in matrix metalloproteinase-13 deficient mice, Biochem. Biophys. Res. Commun. 354 (2007) 846–851.

[48] J. Lecomte, K. Louis, B. Detry, S. Blacher, V. Lambert, S. Bekaert, et al., Bone marrow-derived mesenchymal cells and MMP13 contribute to experimental choroidal neovascularization, Cell Mol. Life Sci. 68 (2011) 677–686.

[49] A. Zijlstra, R.T. Aimes, D. Zhu, K. Regazzoni, T. Kupriyanova, M. Seandel, et al., Collagenolysis-dependent angiogenesis mediated by matrix metalloproteinase-13 (collagenase-3), J. Biol. Chem. 279 (2004) 27633–27645.

[50] Y. Kudo, S. Iizuka, M. Yoshida, T. Tsunematsu, T. Kondo, A. Subarnbhesaj, et al., Matrix metalloproteinase-13 (MMP-13) directly and indirectly promotes tumor angiogenesis, J. Biol. Chem. 287 (2012) 38716–38728.

[51] W. Lederle, B. Hartenstein, A. Meides, H. Kunzelmann, Z. Werb, P. Angel, et al., MMP13 as a stromal mediator in controlling persistent angiogenesis in skin carcinoma, Carcinogenesis 31 (2010) 1175–1184.

[52] K.E. Johnson, T.A. Wilgus, Vascular endothelial growth factor and angiogenesis in the regulation of cutaneous wound repair, Adv. Wound Care (New Rochelle) 3 (2014) 647–661.

[53] A.-K. Olsson, A. Dimberg, J. Kreuger, L. Claesson-Welsh, VEGF receptor signalling? In control of vascular function, Nat. Rev. Mol. Cell Biol. 7 (2006) 359–371.

[54] J. Street, M. Bao, L. deGuzman, S. Bunting, F.V. Peale Jr., N. Ferrara, et al., Vascular endothelial growth factor stimulates bone repair by promoting angiogenesis and bone turnover, Proc. Natl. Acad. Sci. U. S. A. 99 (2002) 9656–9661.

[55] P. Bao, A. Kodra, M. Tomic-Canic, M.S. Golinko, H.P. Ehrlich, H. Brem, The role of vascular endothelial growth factor in wound healing, J. Surg. Res. 153 (2009) 347–358.

[56] G. Bergers, S. Song, The role of pericytes in blood-vessel formation and maintenance, Neuro-Oncology 7 (2005) 452–464.

[57] A. Armulik, A. Abramsson, C. Betsholtz, Endothelial/pericyte interactions, Circ. Res. 97 (2005) 512–523.

[58] W.B. Saunders, B.L. Bohnsack, J.B. Faske, N.J. Anthis, K.J. Bayless, K.K. Hirschi, et al., Coregulation of vascular tube stabilization by endothelial cell TIMP-2 and pericyte TIMP-3, J. Cell Biol. 175 (2006) 179–191.

[59] A.N. Stratman, K.M. Malotte, R.D. Mahan, M.J. Davis, G.E. Davis, Pericyte recruitment during vasculogenic tube assembly stimulates endothelial basement membrane matrix formation, Blood 114 (2009) 5091–5101.